Proceedings of the
47th IEEE Conference on Decision and Control
Cancun, Mexico, Dec. 9-11, 2008

Flight Control of a Rotary wing UAV - A Practical Approach

Bilal Ahmed, Hemanshu R. Pota and Matt Garratt

Abstract— **This paper presents a novel application of the two-time scale controller for the full envelop flight control of a Rotary wing Unmanned Aerial Vehicle (RUAV). In this paper flapping and servo dynamics, important from a practical point of view, is included in the RUAV model. The two-time scale controller takes advantage of the 'decoupling' of the nonlinear translational and rotation dynamics of the rigid body, resulting in a two-level hierarchical control scheme. The inner loop controller (attitude control) tracks the attitude commands and sets the main rotor thrust vector, while the outer loop controller (position control) tracks the reference position and control the flapping angles and the tail rotor thrust vector. High fidelity RUAV simulation results are used to demonstrate the control performance. Simulation results show acceptable performance of the proposed two-time scale controller. The comparison of control inputs between the proposed two-time scale controller and an already implemented PID controller show that this controller is suitable for practical implementation.**

Index Terms— **Robotics, RUAV model, Backstepping, Position control, Lyapunov methods, RUAV simulation**

I. Introduction

This paper presents a position and attitude controller for a rotary wing UAV (RUAV) using two-time scale method. This paper includes the flapping dynamics and the servo actuator dynamics from a practical point of view. The overall objective of this research is the launch and recovery of RUAVs on moving platform. The proposed algorithm considers a full envelop flight control including hover and forward flight condition.

The landing of a RUAV using tether as a guiding mechanism is proposed in [1]. In [1] 'small effects' due to rigidity of the blades are ignored [2]; flapping angles are considered as control inputs resulting in impractical RUAV control inputs. Flapping angles of a RUAV cannot be set directly because of the flapping and the flybar dynamics. Also, servo actuator dynamics play a vital role as mentioned in [3] and essentially it increases the DOF of the system, which is an important consideration for the controller design of an underactuated mechanical system.

The modelling of RUAVs is described in [4]. The design of linear controllers for RUAVs are proposed using LQG [5], H_2 [6], H_∞ [7], μ-synthesis [8] and dynamics inversion [9] methods. A selected literature review relating to the nonlinear control design techniques includes approximate input-output linearization [10], differential flatness [11], sliding mode [12], backstepping [13], [14], [15], neural-network based controller [16], fuzzy control [17] and nonlinear H_∞ control [18].

The innovation in this paper is the extension of the control algorithm in providing a *correction* for the flapping and the servo dynamics. In this paper, a practical approach is presented to control the flapping dynamics indirectly. The method in this paper is proposed with a view to practical implementation on our RUAV based on the Hirobo Eagle RC helicopter [1], [19, Fig. 1].

The organization of this paper is as follows. In Section II, an overview of the nonlinear RUAV model is presented. The servo actuator dynamics is presented in Section III. In Section IV, two-time scale flight control of a RUAV is discussed. This section also discusses a correction control to include flapping dynamics in the attitude control loop. The simulation results are given in Section V, and Section VI presents conclusion of this paper.

II. RUAV Model

This section introduces the basic system blocks which make up the complete dynamics of the RUAV as shown in Fig. 1. This model is based on the nonlinear rigid body dynamics [11], where forces and moments due to main rotor, tail rotor, fuselage and empennage are acting on the center of mass of the body. The position of the origin of the body is denoted by $\zeta = [x, y, z]^T$ in the inertial frame. Linear velocities along the axes of the body frame are given by $V = [u, v, w]^T$. The angular velocity expressed in the body frame is defined as $\omega = [p, q, r]^T$. The Euler angles denoted as $\eta = [\phi, \theta, \psi]^T$ establish a kinematic relationship with the angular velocities $\dot{\eta} = \pi\omega$, where π is given in [15].

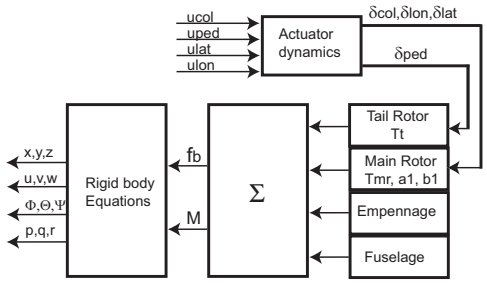

Fig. 1. Schematic of Rotary wing UAV dynamics

Assumption 1 *Euler angles are used in the model to represent the geometric coordinates. This representation has a geometric singularity at $\theta = \pm 90$ deg. It is assumed that the flight condition never reaches this singularity condition.*

B. Ahmed and H.R. Pota are with the School of Information Technology and Electrical Engineering and M. Garratt is with the School of Aerospace, Civil and Mechanical Engineering, The University of New South Wales at the Australian Defence Force Academy, Canberra ACT 2600, Australia, b.ahmed@y7mail.com, h-pota@adfa.edu.au, m.garratt@adfa.edu.au

A brief description of the each sub-system shown in Fig. 1 is given as follows:

A. Rigid-Body Dynamics

The nonlinear rigid-body dynamics in terms of translational and rotational dynamics of the airframe is given by:

$$\dot{\zeta} = V \quad (1)$$
$$m\dot{V} = mge_3 + Rf_b \quad (2)$$
$$\dot{\eta} = \pi\omega \quad (3)$$
$$I\dot{\omega} = -\omega \times I\omega + M \quad (4)$$

where I is the inertia matrix, m is the mass of the body and $R \in SO(3)$ is a rotation matrix between the body and the inertial frame. The parameterized R in terms of the Euler angles is given in [20]. The gravitational force mge_3 is explicitly included where e_3 is a unit vector with one in the third place. Note that the external forces $f_b = [X, Y, Z]^T$ and moments $M = [L, R, N]^T$ are acting on the center of mass of the body due to main and tail rotor, fuselage and empennage.

B. Main and Tail rotor

The main rotor blade flapping a_1, b_1 and the main and tail rotor thrusts T_{mr}, T_t create appropriate forces and moments on the (RUAV) rigid body. The compilation of the forces and moments due to the main and the tail rotor of a RUAV are given as follows [21]:

$$\begin{bmatrix} X_m \\ Y_m \\ Z_m \end{bmatrix} = \begin{bmatrix} -T_{mr}a_1 \\ T_{mr}b_1 + T_t \\ -T_{mr} \end{bmatrix} \quad (5)$$

$$\begin{bmatrix} L_m \\ R_m \\ N_m \end{bmatrix} = \begin{bmatrix} \frac{dL}{db_1}b_1 + Y_m.M_Z + Tt.T_Z \\ \frac{dM}{da_1}a_1 + X_m.M_Z \\ M_Q + Y_m.M_X + Tt.T_X \end{bmatrix} \quad (6)$$

The main rotor torque M_Q can be computed using an approximation given in [22]. Note that there exists algebraic relationships between T_{mr} and δ_{col} and also between T_t and δ_{ped} [20, p. 1958].

First order flapping dynamics for the Eagle RUAV is given by:

$$\dot{a}_1 = -\frac{a_1}{\tau_f} + q + \frac{A_c}{\tau_f}c + \frac{A_{lon}}{\tau_f}\delta_{lon} \quad (7)$$
$$\dot{b}_1 = -\frac{b_1}{\tau_f} - p + \frac{B_d}{\tau_f}d + \frac{B_{lat}}{\tau_f}\delta_{lat} \quad (8)$$
$$\dot{c} = -\frac{c}{\tau_s} + q + \frac{C_{lon}}{\tau_s}\delta_{lon} \quad (9)$$
$$\dot{d} = -\frac{d}{\tau_s} - p + \frac{D_{lat}}{\tau_s}\delta_{lat} \quad (10)$$

where $\delta_{lat}, \delta_{lon}$ are servo actuator outputs, c, d are flybar flapping angles and τ_f, τ_s are the main rotor flapping and flybar time constants. The identified parameters $A_c, A_{lon}, B_d, B_{lat}, C_{lon}, D_{lat}$ for the Eagle RUAV are given in Table I. Apart from the dominant forces and moments due to the main and tail rotor, relative wind acting on the helicopter produces forces due to the fuselage and vertical/horizontal wings which is given in the next paragraph.

C. Fuselage and Empennage

The forces and moments due to fuselage and empennage are given as follows [23, p. 115]:

$$[X_{fs}, Y_{fs}, Z_{fs}]^T = \frac{\rho}{2}\left[F_{ax}\ u^2, F_{ay}\ v^2, F_{az}\ w^2\right]^T \quad (11)$$
$$[L_{fs}, R_{fs}, N_{fs}]^T = [0, 0, 0]^T \quad (12)$$
$$[X_v, Y_v, Z_v]^T = [0, F_{vt}, 0]^T \quad (13)$$
$$[L_v, R_v, N_v]^T = [F_{vt}\ vt_x, 0, F_{vt}\ vt_z]^T \quad (14)$$

where F_{ax}, F_{ay}, F_{az} are the coefficients of the drag force relative to the center of gravity of the body and F_{vt} is an aerodynamic force due to vertical tail.

Forces $f_b = [X, Y, Z]^T$ and moments $M = [L, R, N]^T$ in (2) and (4) are obtained by putting together (5)–(6) and (11)–(14) given by:

$$X = X_m + X_{fs} + X_v \quad (15)$$
$$Y = Y_m + Y_{fs} + Y_v \quad (16)$$
$$Z = Z_m + Z_{fs} + Z_v \quad (17)$$
$$L = L_m + L_{fs} + L_v \quad (18)$$
$$R = R_m + R_{fs} + R_v \quad (19)$$
$$N = N_m + N_{fs} + N_v \quad (20)$$

III. Servo Actuator Dynamics

Radio controlled servo actuators are an essential part of RUAVs. Servo dynamics sets a constraint in designing a controller due to delay and rate limitation. The delay and rate limit due to servo actuators degrade the stability margin and hence this needs to be considered during the control system design. To model the servo (JR DS8231) dynamics separately and to explicitly include the rate limit, experiments were conducted on servo actuators with a sinusoidal chirp as the test input as shown in the Fig. 2. Apart from rate limitation, the first pole which occurs at about 5Hz imposes a bandwidth limitation in designing a controller. The frequency response, at different input signal amplitudes, is shown in Fig. 3.

The first order servo actuator model is given by:

$$\dot{\delta}_i = -\tau_i\delta_i + u_i \quad (21)$$

where $i = lat, lon$; the time constant τ_i is $0.04\ sec.$ A rate limitation for the input u_i is set to $\pm 2.5\ deg$ in simulation.

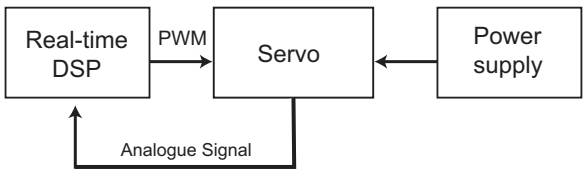

Fig. 2. Block diagram of the radio controlled servo actuator identification

Assumption 2 *The Eagle platform is equipped with fast digital servos (NES-8700G) for the tail rotor pitch control*

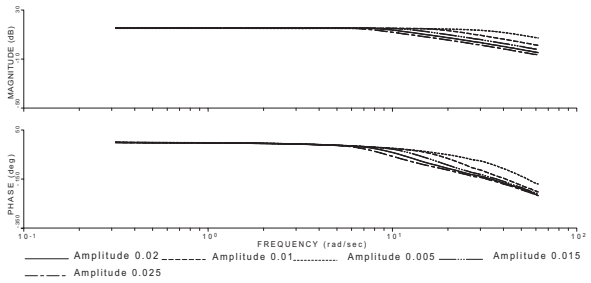

Fig. 3. Frequency response of DS8231 servo actuator

with active yaw damping system. It is assumed that the servo dynamics is much faster than the main and the tail rotor pitch control $\delta_{col}, \delta_{ped}$. The servo actuator dynamics for the cyclic pitch control $\delta_{lat}, \delta_{lon}$ is comparable with that of the flapping dynamics a_1, b_1, c, d.

IV. Two-time Scale Control

The aim of this section is to present a two-time scale controller, which essentially makes use of separation in the nonlinear translational and rotational dynamics of the RUAV. The block diagram of the closed-loop system is shown in Fig. 4. Two-level hierarchical control scheme contains an

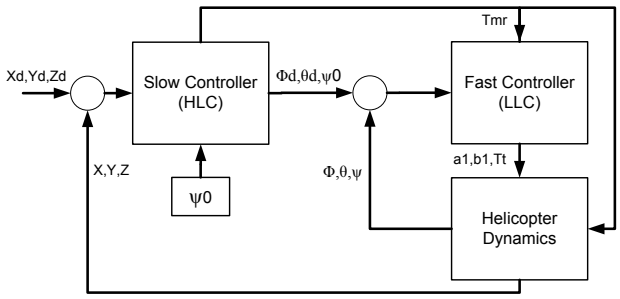

Fig. 4. Two-time scale-based full envelop flight control of a RUAV

inner loop fast controller (attitude control) and an outer loop slow controller (position control). The main idea is to compute the control inputs to achieve the desired thrust and flapping angles for the commanded position. The proposed control law is elaborated in the following paragraphs.

A. Design of an Attitude Controller

The rigid-body rotational dynamics from (3)–(4) and the flapping dynamics from (7)–(10) including servo dynamics is given below for easy reference:

$$\dot{\eta} = \pi\omega \tag{22}$$
$$I\dot{\omega} = -\omega \times I\omega + M \tag{23}$$
$$\dot{a}_1 = -\frac{a_1}{\tau_f} + q + \frac{A_c}{\tau_f}c + \frac{A_{lon}}{\tau_f}\delta_{lon} \tag{24}$$
$$\dot{b}_1 = -\frac{b_1}{\tau_f} - p + \frac{B_d}{\tau_f}d + \frac{B_{lat}}{\tau_f}\delta_{lat} \tag{25}$$
$$\dot{c} = -\frac{c}{\tau_s} + q + \frac{C_{lon}}{\tau_s}\delta_{lon} \tag{26}$$
$$\dot{d} = -\frac{d}{\tau_s} - p + \frac{D_{lat}}{\tau_s}\delta_{lat} \tag{27}$$
$$\dot{\delta}_{lat} = -\tau_{lat}\delta_{lat} + u_{lat} \tag{28}$$
$$\dot{\delta}_{lon} = -\tau_{lon}\delta_{lon} + u_{lon} \tag{29}$$

The control objective in this section is to design a control law $u = [u_{lat}, u_{lon}, \delta_{ped}]$ for the system (22)–(29) to track the desired attitude $\eta_d = [\phi_d, \theta_d, \psi_d]$. To achieve this objective, a nonlinear design technique called backstepping [24] is used in this paper. As a first step in using backstepping, let the starting Lyapunov Function Candidate (LFC) be:

$$W_1 = \frac{1}{2}(\eta - \eta_d)^T K_\eta (\eta - \eta_d)$$

where K_η is a positive definite matrix. The desired attitude $\eta_d = [\phi_d, \theta_d, \psi_d]$ is a reference signal generated by the position controller then,

$$\dot{W}_1 = (\pi\omega)^T K_\eta \tilde{\eta} \tag{30}$$

If

$$\omega = \omega^d \triangleq -\alpha\pi^{-1}\tilde{\eta} \;\; (\alpha \; is \; scalar \; \alpha > 0) \tag{31}$$

where $\tilde{\eta} = (\eta - \eta_d)$ then $\dot{W}_1 \leq 0$. Let us denote $\pi^{-1} = \gamma$ in (31) for notational simplicity. The process of backstepping continues by defining an error $z_1 \triangleq \omega - \omega^d$ and having another LFC as follows:

$$W_2(\eta, z_1) = \frac{1}{2}(\eta - \eta_d)^T K_\eta (\eta - \eta_d) + \frac{1}{2} z_1^T I z_1$$

then,

$$\dot{W}_2 = z_1^T\left(\pi^T K_\eta \tilde{\eta} - \omega \times I\omega + M + \alpha I\gamma\dot{\eta} + \alpha I\dot{\gamma}\tilde{\eta}\right) + \underbrace{(\pi\omega^d)^T K_\eta \tilde{\eta}}_{\leq 0} \tag{32}$$

If

$$M = \omega \times I\omega - \alpha I\gamma\dot{\eta} - \alpha I\dot{\gamma}\tilde{\eta} - \pi^T K_\eta \tilde{\eta} \tag{33}$$

then $\dot{W}_2 \leq 0$.

Remark 1 The inputs to the attitude controller are the desired attitude η_d and a nominal value of the main rotor thrust $\bar{T}_{mr}$. To achieve the desired attitude the moments M

should be as given by (33). This value of M is achieved by setting a_1, b_1, T_t such that (18)–(20) are satisfied.

The flapping angles a_1, b_1 can only be controlled indirectly, thus a feedback system is used to minimize an *error* between the actual flapping angles and the desired flapping angles. The flapping angles can be obtained by using the following rotor moment formulation [4] given by:

$$\dot{p} = K_\beta b_1 \quad (34)$$
$$\dot{q} = -K_\beta a_1 \quad (35)$$

Remark 2 Commercially-Off-The-Shelf (COTS) rate gyros are used to measure the angular velocities $\omega = [p, q, r]^T$ of the Eagle RUAV. We have calculated the roll-acceleration $\dot{p}$ and pitch-acceleration $\dot{q}$ by differentiating the measured angular velocities and using the accelerations to estimate the flapping angles a_1, b_1.

The flapping error dynamics using (24)–(29) can be written as,

$$\dot{X}_e = A_e X_e + B_e \tilde{u} \quad (36)$$

where,

$$X_e = [a_1 - a_1^d, b_1 - b_1^d, c - c^d, d - d^d, \delta_{lat} - \delta_{lat}^d, \delta_{lon} - \delta_{lon}^d, p, q]^T$$
$$\tilde{u} = \left[u_{lat} - u_{lat}^d, u_{lon} - u_{lon}^d\right]^T$$

The steady-state control inputs u_{lon}^d, u_{lat}^d can be obtained by setting $\dot{a}_1, \dot{b}_1, \dot{c}, \dot{d}, \dot{\delta}_{lat}, \dot{\delta}_{lon} = 0$ in (24)–(29). Let us choose a system LFC given by:

$$W_3(\eta, z_1, X_e) = W_2 + X_e^T P X_e, \quad (37)$$

where P is a positive definite matrix. Let $M = U_m^d + \tilde{U}_m$, where U_m^d is the value of the right-hand side of (33) with a_1^d, b_1^d, T_t^d and $\tilde{U}_m$ is yet to be computed "correction" term which is chosen to make $\dot{W}_3$ in the presence of flapping dynamics negative definite. When the flapping dynamics is ignored $\tilde{U}_m = 0$. The time derivative of (37) along the system trajectories is then given by:

$$\dot{W}_3 = \dot{W}_2 + z_1^T \tilde{U}_m + X_e^T \left(A_e^T P + A_e P\right) X_e + [\tilde{u}_{lat}, \tilde{u}_{lon}] \left(B_e^T P + B_e^T P^T\right) X_e \quad (38)$$

$\dot{W}_3$ can shown to be non-positive by considering three separate cases:

1) X_e *equals to zero*: In this case $\tilde{U}_m$ is zero because the actual flapping angles are at their desired values. The control signal U_m^d will make $\dot{W}_3 = 0$.
2) X_e *is non-zero and* $B_e^T P + B_e^T P^T$ *is not orthogonal to* X_e: In this case choose $\tilde{u} = K X_e$, where K is fixed gain matrix. Substituting this in (38) gives:

$$\dot{W}_3 = \dot{W}_2 + z_1^T \tilde{U}_m + \underbrace{X_e^T \left[(A_e + B_e K)^T P + P (A_e + B_e K)\right] X_e}_{\leq 0 \text{ for suitable } K}$$

It is possible to make the $\dot{W}_2 + z_1^T \tilde{U}_m$ term non-positive by choosing control as given in Proposition 1 below.

3) $\left(B_e^T P + B_e^T P^T\right) X_e = 0$ In this case Proposition 1 can be used to introduce the tail rotor thrusts to set $\dot{W}_3 = 0$

Proposition 1 *When* $\left(B_e^T P + B_e^T P^T\right) X_e = 0$ *the tail rotor thrust* $T_t^d = T_t + \tilde{T}_t$ *can be chosen such that* $\dot{W}_3 = 0$, *provided* $z_1(1) \neq 0$ *or* $z_1(3) \neq 0$.

Proof: The derivative of the LFC is given by:

$$\dot{W}_3 = \dot{W}_2 + z_1^T \tilde{U}_m + X_e^T \left(A_e^T P + A_e P\right) X_e \quad (39)$$

In the above equation, choose P a positive definite such that $\left(A_e^T P + A_e P\right)$ is negative definite. The remaining terms are given by:

$$\Delta \dot{W}_3 = \dot{W}_2 + z_1^T \tilde{U}_m \quad (40)$$

where, Δ denotes the remaining terms from (39). Note that, $M = U_m^d + \tilde{U}_m$ and in terms of $\bar{T}_{mr}, a_1, b_1, T_t$. Note that $\bar{T}_{mr}$ is a nominal value from the position controller.

Remark 3 The idea here is to choose the tail rotor thrust T_t to make $\Delta \dot{W}_3 = 0$, if there are no control inputs available due to higher DOF.

The $\tilde{U}_m$ is given by:

$$\tilde{U}_m = \begin{bmatrix} \frac{dL}{db_1}\tilde{b}_1 + (\bar{T}_{mr}\tilde{b}_1 + \tilde{T}_t)Mz + \tilde{T}_t Tz \\ \frac{dM}{da_1}\tilde{a}_1 - \bar{T}_{mr}\tilde{a}_1 Mz \\ \bar{T}_{mr}\tilde{b}_1 Mx + \tilde{T}_t Mx + \tilde{T}_t Tx \end{bmatrix}$$

The leftover terms (40) are given by:

$$\Delta \dot{W}_3 = \dot{W}_2 + z_1^T \tilde{U}_m = \dot{W}_2 + \chi_1^T z_1 + \bar{T}_{mr}(\chi_2^T z_1) + \tilde{T}_t(\chi_3^T z_1)$$

where,

$$\chi_1 = \begin{bmatrix} \tilde{b}_1(\frac{dL}{db_1} + \bar{T}_{mr}Mz) \\ \tilde{a}_1(\frac{dM}{da_1} - \bar{T}_{mr}Mz) \\ 0 \end{bmatrix} \chi_2 = \begin{bmatrix} 0 \\ 0 \\ \tilde{b}_1 Mx \end{bmatrix}$$
$$\chi_3 = \begin{bmatrix} Mz + Tz \\ 0 \\ Mx + Tx \end{bmatrix}$$

The tail rotor thrust $\tilde{T}_t$ can be chosen in the following manner to make $\Delta \dot{W}_3 = 0$.

$$\tilde{T}_t = \frac{-\chi_1^T z_1 - \bar{T}_{mr}\chi_2^T z_1}{\chi_3^T z_1} \quad (41)$$

provided $z_1(1) \neq 0$ or $z_1(3) \neq 0$.

The above condition shows that it is possible to stabilized the complete system even when $(B_e^T P + B_e^T P^T)X_e = 0$. The above results are novel and can be used in other control applications for the underactuated mechanical systems.

B. Design of an Position Controller

The translational dynamics of the system from (1)–(2) and (21) is given by:

$$\dot{\zeta} = V \quad (42)$$

$$m\dot{V} = mge_3 + Rf_b \quad (43)$$

The control objective in this section is to design a control law $u = [\phi_d, \theta_d, \delta_{col}]$ for the system (42)–(43) to track the desired position $\zeta_d = [x_d, y_d, z_d]$.

Proposition 2 *If a tracking error exist between η and η_d, then the attitude converged to the last command $\eta = \eta_d$ and a_1, b_1, T_t converged to the desired values $\bar{a}_1, \bar{b}_1, \bar{T}_t$.*

Proof: See [1, p. 540]

The backstepping technique can be used for the given system because of its feedback form. The process starts by having a LFC as follows:

$$W_4 = \frac{1}{2}(\zeta - \zeta_d)^T(\zeta - \zeta_d),$$

where ζ_d is a constant then

$$\dot{W}_4 = (\zeta - \zeta_d)^T V \quad (44)$$

If

$$V_d = -\frac{1}{m}(\zeta - \zeta_d) \quad (45)$$

then

$$\dot{W}_4 = -\frac{1}{m}(\zeta - \zeta_d)^T(\zeta - \zeta_d) \leq 0$$

The process of backstepping continues by defining an 'error' ($z_2 \stackrel{\triangle}{=} mV - mV_d$) and choosing a system LFC given by:

$$W_5 = \frac{1}{2}(\zeta - \zeta_d)^T(\zeta - \zeta_d) + \frac{1}{2}z_2^T z_2$$

then

$$\dot{W}_5 = \underbrace{(\zeta - \zeta_d)^T V_d}_{\leq 0} + (\zeta - \zeta_d)^T z_2 + z_2^T(Rf_b + mge_3 + V)$$

If

$$Rf_b = -K_p(\zeta - \zeta_d) - K_d V - mge_3 \quad (46)$$

where, K_p, K_d are diagonal gain matrices and $K_p, K_d \geq 0$ then $\dot{W}_5 \leq 0$.

Assumption 3 *It is assumed that the desired heading ψ_d is a constant value ψ_0 and provided by the user. This assumption is valid because ψ will converged to ψ_0 in the attitude control loop and it enables pilot to set the desired heading.*

Remark 4 The forces f_b in (46) are in terms of $\bar{a}_1, \bar{b}_1, \bar{T}_t, T_{mr}$ given in (15)–(17). Note that at this stage $\bar{a}_1, \bar{b}_1, \bar{T}_t$ are the desired values. This leads to the solution of three nonlinear algebraic equations for ϕ, θ, T_{mr} using (46) and (15)–(17). The nonlinear equations are solved using the Newton-Raphson method with initial condition $[0, 0, -80]$ and solution converged after 10 iterations.

TABLE I
PARAMETERS OF THE EAGLE RUAV

Parameter	Description
m = 8.2 Kg	helicopter mass
I_{xx}, I_{yy}, I_{zz} = 0.23,0.82,0.4 Kg.m^2	Inertia components
M_x, M_z = 0,-0.284	Main rotor distances w.r.t C.G.
T_x, T_z = -0.915,-0.104	Tail rotor distances w.r.t C.G.
K_β =270	Main rotor hub spring constant
τ_s, τ_f = 0.226, 0.027 sec	Flapping time constants
A_c, B_d= 0.152,0.136 rad/ms	Bell-mixer derivative
A_{lon}, B_{lat} = 0.19,0.17 rad/ms	Stick to swash-plat gearings
C_{lon}, D_{lat} = 1.58,1.02 rad/ms	Stick to swash-plate gearings

V. SIMULATION

Performance of the controller is tested using a high fidelity RUAV simulation [25] including flapping dynamics. The two-time scale controller simulation results are shown in Fig. 5. Simulation is done for the case where the initial position $\zeta = [-5.0, 0, -2]^T$ and the desired position $\zeta_d = [-5.0, -1.0, -4.0]^T$. The control inputs obtained using two-time scale controller are compared with a PID controller in Fig. 5. Note that the same initial and desired positions are used for the PID controller and the proposed two-time scale controller in this simulation. The proposed controller shows control input values suitable for practical implementation.

VI. CONCLUSION

In this paper, a position control of a RUAV is presented including the flapping and the servo actuator dynamics. The proposed controller is based on two-level hierarchical control scheme, i.e, inner loop attitude control and outer loop position control. The simulation results confirm the asymptotic stability of the position and attitude control loops. This paper contributes novel results in presenting a detailed analysis of the flapping correction dynamics which is an essential part for the control implementation purposes on RUAVs. The RUAV model presented in this paper is based on the minimum complexity helicopter model, but captures the key dynamics of the platform. Work is in progress to implement the proposed controller on our Eagle RUAV.

REFERENCES

[1] S. Oh, K. Pathak, S. Agrawal, H. Pota, and M. Garratt, "Approaches for a tether-guided landing of an autonomous helicopter," *IEEE Transactions on Robotics*, vol. 22, no. 3, pp. 536–544, 2006.

[2] K. Pathak and S. Agrawal, "An Integrated Spatial Path-planning and Controller Design Approach for a Hover-mode Helicopter Model," in *IEEE Conference on Robotics and Automation*, April 2005, pp. 1890–1895.

[3] A. Calise, H. Lee, and N. Kim, "High Bandwidth Adaptive Flight Control," in *AIAA Conference on Guid., Navig., and Control*, August 2000.

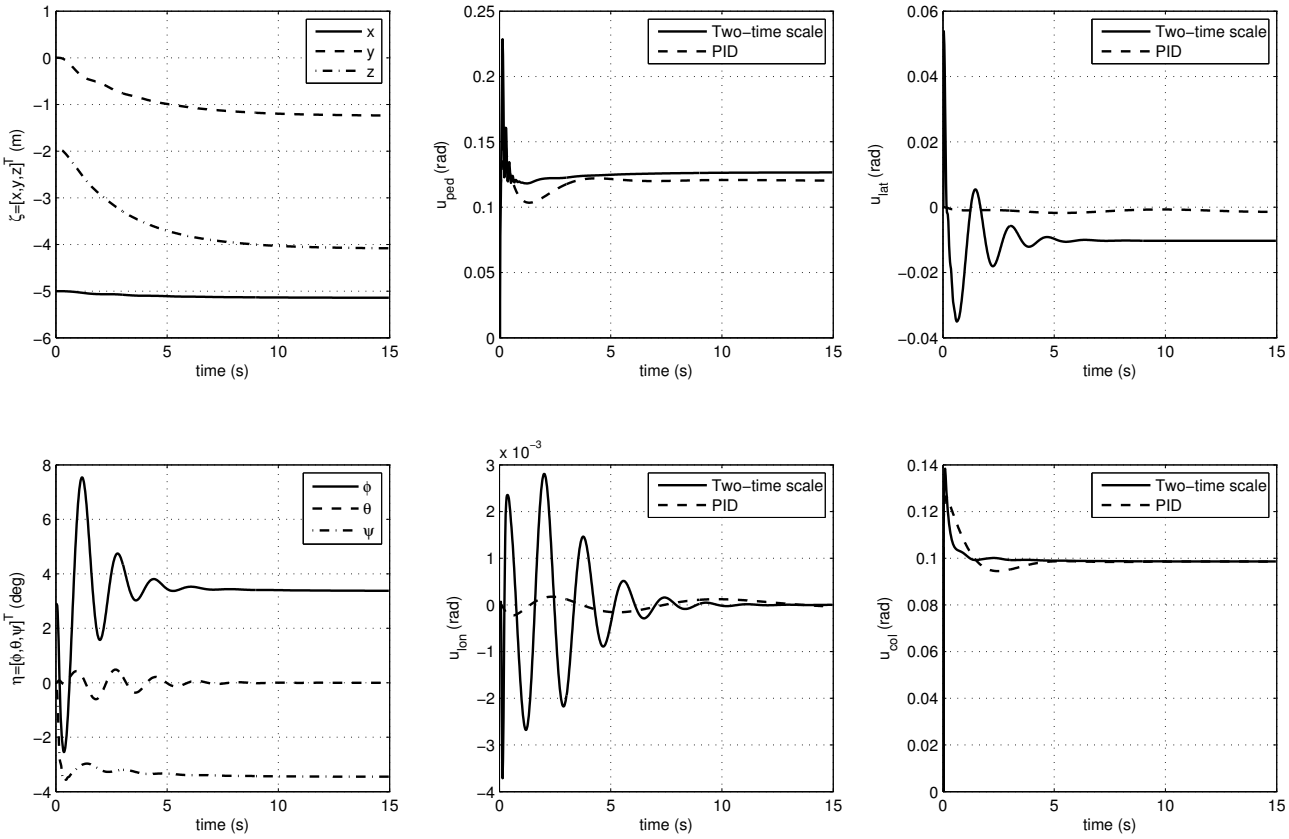

Fig. 5. Simulation results of the two-time scale controller at sampling time 0.02 sec.

[4] V. Gavrilets, B. Mettler, and E. Feron, "Nonlinear model for a small-size acrobatic helicopter," in *AIAA Conference on Guid., Navig., and Control*, Montreal, Quebec, Canada, August 2001.

[5] J. Morris, M. Van Nieuwstadt, and P. Bendotti, "Identification and control of a model helicopter in hover," in *Proceedeings of the American Control Conference*, vol. 2, June 1994, pp. 1238–1242.

[6] M. Takahashi, "Synthesis and evaluation of an H_2 control law for a hovering helicopter," *J. Guid., Control, Dyn.*, vol. 16, no. 3, pp. 579–584, 1993.

[7] H. Shim, T. Koo, F. Hoffmann, and S. Sastry, "A comprehensive study of control design for an autonomoushelicopter," in *IEEE Conference on Decision and Control*, vol. 4, December 1998.

[8] G. Dudgeon and J. Gribble, "Helicopter attitude command attitude hold using individual channel analysis and design," *J. Guid., Control, Dyn.*, vol. 20, no. 5, 1997.

[9] S. Snell and P. Stout, "Robust longitudinal control design using dynamic inversion and quantitative feedback theory," *J. Guid., Control, Dyn.*, vol. 20, no. 5, pp. 933–940, 1997.

[10] R. Mahony and R. Lozano, "(Almost) exact path tracking control for an autonomous helicopter in hover manoeuvres," in *IEEE Conference on Robotics and Automation*, 2000, pp. 1245–1250.

[11] T. Koo and S. Sastry, "Output tracking control design of a helicopter model based on approximate linearization," in *IEEE Conference on Decision and Control*, vol. 4, December 1998, pp. 3635–3640.

[12] J. Pieper, "Application of SLMC: TRC control of a helicopter in hover," in *Proceedeings of the American Control Conference*, June 1995, pp. 1191–1195.

[13] R. Mahony and T. Hamel, "Robust trajectory tracking for a scale model autonomous helicopter," *Journal of Robust Nonlinear Control*, vol. 14, pp. 1035–1059, 2004.

[14] H. Pota, B. Ahmed, and M. Garratt, "Velocity control of a UAV using backstepping control," in *IEEE Conference on Decision and Control*, San Diego, CA, USA, 13–15 December 2006, pp. 5894–5899, ISBN 1-4244-0342-1.

[15] B. Ahmed and H. Pota, "Backstepping-based landing control of a RUAV using tether incorporating flapping correction dynamics," in *Proceedeings of the American Control Conference*, Seattle, Washington, USA, June 2008, pp. 2728–2733, ISBN 1-4244-2079-7.

[16] J. Prasad, A. Calise, Y. Pei, and J. Corban, "Adaptive nonlinear controller synthesis and flight test evaluation," in *IEEE Conference on Control Applications*, 1999, pp. 137–142.

[17] C. Sanders, P. DeBitetto, E. Feron, H. Vuong, and N. Leveson, "Hierarchical control of small autonomous helicopters," in *IEEE Conference on Decision and Control*, vol. 4, December 1998, pp. 3629–3634.

[18] C. Yang, W. Liu, and C. Kung, "Nonlinear H_∞ decoupling control for hovering helicopter," in *Proceedeings of the American Control Conference*, May 2002, pp. 4353–4358.

[19] M. Garratt, B. Ahmed, and H. Pota, "Platform enhancements and system identification for control of an unmanned helicopter," in *IEEE Conference on Control, Aut., Robotics and Vision — ICARCV 2006*, Singapore, 5–8 December 2006, pp. 1981–1986, ISBN 1-4244-0342-1.

[20] B. Ahmed, H. Pota, and M. Garratt, "Rotary wing UAV position control using backstepping," in *IEEE Conference on Decision and Control*, New Orleans, LA, USA, December 2007, pp. 1957–1962, ISBN 1-4244-1498-9.

[21] R. Prouty, *Helicopter Performance, Stability, and Control*. PWS Engineering, 1986.

[22] T. Koo and S. Sastry, "Differential flatness based full authority helicopter control design," in *IEEE Conference on Decision and Control*, vol. 2, December 1999, pp. 1982–1987.

[23] G. Padfield, *Helicopter flight dynamics: The theory and application of flying qualities and simulation modeling*. AIAA, 1996.

[24] H. Khalil, *Nonlinear Systems*, 3rd ed. Englewoo Cliffs, NJ: Prentice Hall, 2002.

[25] M. Garratt, "Biologically inspired vision and control for an autonomous flying vehicle," Ph.D. dissertation, Australian National University, October 2007.